Bond-located ordering in the one-dimensional Penson - Kolb - Hubbard model

1997 J. Phys.: Condens. Matter 9 10509

(http://iopscience.iop.org/0953-8984/9/47/018)

J. Phys.: Condens. Matter **9** (1997) 10509–10519. Printed in the UK PII: S0953-8984(97)84992-2

Bond-located ordering in the one-dimensional Penson–Kolb–Hubbard model

G I Japaridze† and E Müller-Hartmann

Institut für Theoretische Physik, Univ. zu Köln, Zülpicher Straße 77, Köln 50937, Germany

Received 6 June 1997

Abstract. In this paper we study the ground-state phase diagram of the one-dimensional half-filled repulsive ($U > 0$) Hubbard model supplemented with the pair-hopping interaction (W) (the Penson–Kolb–Hubbard model) using the continuum-limit field theory approach. We compare the low-energy properties of the $U > 0$ Hubbard model and $W > 0$ Penson–Kolb model. We show that, despite similar excitation spectra, the character of instabilities in these models is completely different. In contrast to the Hubbard model, in the case of the Penson–Kolb model, the dynamical generation of a charge gap leads to the suppression of spin-density-wave (SDW) fluctuations. The charge-density-wave fluctuations survive and coexist with bond-located SDW (Bd-SDW) instabilities. The Bd-SDW corresponds to a magnetically ordered state with staggered magnetization located on bonds between sites. The possibility of bond-located ordering is connected with the site-off-diagonal nature of the pair-hopping interaction. In the case of PKH the bond-ordered states exist at $|W| > U/2$. For $W > U/2$ the Bd-SDW is realized while for $W < -U/2$ the dimerized phase is realized.

1. Introduction

Since the discovery of high-temperature superconductivity a great variety of different pairing mechanisms has been proposed. Many of these proposals contain the concept of pairing in real space as far as the 'Cooper pairs' observed in high-T_c materials are characterized by the extremely small coherence lengths in marked contrast to traditional (BCS) superconductors. The attractive ($U < 0$) Hubbard model

$$\mathcal{H} = -t \sum_{n,\alpha} (c^{\dagger}_{n,\alpha} c_{n+1,\alpha} + c^{\dagger}_{n+1,\alpha} c_{n,\alpha}) + U \sum_{n} c^{\dagger}_{n,\uparrow} c_{n,\uparrow} c^{\dagger}_{n,\downarrow} c_{n,\downarrow} \tag{1}$$

was often considered to describe the evolution from the BCS-type pairing to the local pair (composite boson) limit (see for a review see [1]). A rather different realization of a pairing in real space is the η-pairing mechanism of superconductivity introduced by Yang [2] for the Hubbard model. Yang discovered a class of eigenstates of the Hubbard Hamiltonian which have the property of off-diagonal long-range order, which in turn implies the Meissner effect and flux quantization [3–5], i.e. superconductivity. These eigenstates are constructed in terms of doubly occupied sites ('Cooper pairs' of zero size) with momentum π. Yang also proved that these states cannot be ground states for the Hubbard model with finite interaction. η-superconductivity is realized in the Hubbard model only at infinite on-site attraction [6]. Later several generalizations of the Hubbard model, showing η-superconductivity in the ground state (for a finite on-site interaction) were proposed [7–11].

† Permanent address: Institute of Physics, Georgian Academy, Tamarashvili 6, Tbilisi, 380077 Georgia. E-mail address: gijapa@physics.iberiapac.ge

0953-8984/97/4710509+11$19.50

Another model which captures the essential physics of both above-mentioned scenarios for the realization of pairing in real space, is the Penson–Kolb (PK) model [12]. The Hamiltonian of the PK model contains, in addition to the usual one-electron hopping term, a term that hops singlet pairs of electrons from site to site and in the one-dimensional case is given by

$$\mathcal{H} = -t \sum_{n,\alpha} (c^{\dagger}_{n,\alpha} c_{n+1,\alpha} + c^{\dagger}_{n+1,\alpha} c_{n,\alpha}) + W \sum_{n} (c^{\dagger}_{n,\uparrow} c^{\dagger}_{n,\downarrow} c_{n+1,\downarrow} c_{n+1,\uparrow} + \text{h.c.}). \tag{2}$$

In the case of *negative* W the PK model describes a continuous evolution of the usual BCS-type superconducting state at $|W| \ll t$ into a local pair superconducting limit at $|W| \gg t$ [13]. In the case of large *positive-W* ($W > W_c \simeq 2t$) the ground state of the PK model is η-superconducting [14, 15]. The rich and unusual phase diagram of the PK model has triggered considerable interest, of late, to models with pair-hopping interaction [13–21].

It is notable that the pair-hopping term (though introduced phenomenologically) and the Hubbard term, could be obtained from the same general tight-binding Hamiltonian [22] by approximating the two-particle coupling. Indeed the same matrix element of the electron–electron interaction potential $V(r)$,

$$V(n, m, k, l) = \int \mathrm{d}r \, \mathrm{d}r' \, \rho_{nl}(r) \rho_{mk}(r') V(r - r') \tag{3}$$

which gives rise to the on-site Hubbard interaction for $n = m = k = l$ leads to the pair-hopping amplitude W for $n = m$ and $k = l = n \pm 1$. In equation (3), ρ_{ij} denotes the matrix element of the electron-density operator, $\hat{\rho}(r)$, in the Wannier representation $\rho_{ij}(r) = \Phi^{*}_{i} \Phi_{j}$. Although originating from the same two-body potential the Hubbard and the pair-hopping couplings represent different types of correlations in the electron system. If the Hubbard term describes on-site correlations, the site-off-diagonal pair-hopping term describes part of the so-called 'bond-charge' interaction [23]. To clarify similarities and differences between these two sources of correlations the comparative study of the Hubbard and PK model is very useful.

As it was shown by Affleck and Marston [13], the attractive ($W < 0$) PK model behaves qualitatively like the attractive Hubbard model. For all $W < 0$ (and for arbitrary band-filling) there is a gap in the spin excitation spectrum, the charge excitation spectrum is gapless and the singlet superconducting (SS) instabilities are most divergent in the ground state. The difference with the $U < 0$ Hubbard model occurs only in the case of the half-filled band. At this particular band-filling the Hubbard model is characterized by the coexistence of charge-density-wave (CDW) and SS instabilities in the ground state [24, 25].

The repulsive ($W > 0$) PK model exhibits a transition into the η-superconducting state at $W > W_c \simeq 2t$ [14, 15]. The transition is of first order (level crossing) and leads to a drastic change in the structure of the ground state: after the transition the one-particle hopping term is almost frozen out [15], the spin excitations are gapped, while the charge excitations are gapless [17]. The critical value W_c weakly depends on the band-filling and varies between $W_c \simeq 1.8t$ at half-filling to $W_c \simeq 2t$ for two particles on the lattice. There is no similarity with the repulsive Hubbard model. The site-off-diagonal nature of the pair-hopping term is crucial in this case [15].

At $0 < W < W_c$ the PK model shares some common features with the repulsive Hubbard model. Namely in the case of non-half-filled band the low-energy behaviour of the PK and Hubbard models is qualitatively similar [13, 18, 15]. Moreover, in the case of the half-filled band the excitation spectrum of the PK model and the $U > 0$ Hubbard model is identical [13, 17]. However, at half-filling the symmetry of instabilities has been the subject of some controversy. The real space renormalization group approach shows

an enhancement of the CDW fluctuations [14], while studies within the Green function formalism [18] show domination of the spin density-wave (SDW) instabilities.

To clarify the particularities appearing in the half-filled band case, in this paper we investigate the weak-coupling ground-state phase diagram of the generalized $(U - W)$ Penson–Kolb–Hubbard (PKH) model using the continuum-limit approach and bosonization technique. We compare the low-energy behaviour of the $W > 0$ PK model with the repulsive Hubbard model. We show that at half-filling the site-off-diagonal nature of the pair-hopping interaction manifests itself pronouncedly already in the weak-coupling limit. In contrast to the Hubbard model, in the PK model generation of the charge gap leads to suppression of the SDW fluctuations. The CDW fluctuations survive. Moreover, an instability with respect to bond-located ordering appears. Namely, the bond-located spin-density-wave (Bd-SDW) phase, with order parameter

$$O_{Bd\text{-SDW}} = (-1)^n \sum_{\alpha} \alpha (c^{\dagger}_{n,\alpha} c_{n+1,\alpha} + c^{\dagger}_{n+1,\alpha} c_{n,\alpha}) \tag{4}$$

describing a staggered magnetization located on bonds between sites is one of the possible ordered states of the half-filled PK model. The possibility of bond-located magnetic ordering was not considered in previous studies and is directly connected with the site-off-diagonal nature of the pair-hopping term. The very presence of the interaction coupled with on-bond degrees of freedom leads to the peculiar ordering inside these degrees of freedom.

In the case of the PKH model the bond-ordered states exist at $|W| > U/2$. For $W > U/2$ the low-energy properties of the PKH model are similar to the $U = 0$ case: coexistence of the CDW and Bd-SDW instabilities. This phase becomes unstable with respect to transition into η-superconducting phase with increasing W. For $W < 0$ the line $|W| = U/2$ corresponds to a transition into the dimerized (Peierls) phase at $|W| < U/2$. Dimerized phase becomes unstable with respect to transition into a singlet superconducting phase with increasing $|W|$.

Our paper is organized as follows. In section 2 we will review the PK model and its symmetries. In section 3 we construct the continuum-limit version of the PKH model and perform a renormalization-group analysis of the corresponding field theory. In section 4 we study the large-scale behaviour of the various correlation functions and compare phase diagrams of $U > 0$ Hubbard model and $W > 0$ PK model. In section 5 the ground-state phase diagram of the PKH model is presented and a summary of the results is given.

2. Review of the Penson–Kolb model and its symmetries

There are two important aspects distinguishing the PK model from the Hubbard model. First is the symmetry of these models, second is the nonlocal character of the pair-hopping interaction.

Let us first consider the symmetry aspect. The PK and Hubbard models are characterized by the same $SU(2)$-spin symmetry. The difference lies in the symmetry of the corresponding charge sectors—$SU(2)$ in the case of half-filled Hubbard model and $U(1)$ in the case of PK model [13]. This can be easily seen in the case of strong interactions.

It is well known that the repulsive Hubbard model at $U \gg t$ is equivalent to the spin-$\frac{1}{2}$ Heisenberg model

$$\mathcal{H} = J \sum_{n} \boldsymbol{S}_n \boldsymbol{S}_{n+1} \tag{5}$$

where $J = t^2/U$. A spin-down particle–hole transformation $c_{n,\downarrow} \to (-1)^n c^{\dagger}_{n,\downarrow}$, changes the

sign of U without affecting t and interchanges charge with spin operators

$$\rho(n) = \sum_{n,\alpha} c^{\dagger}_{n,\alpha} c_{n,\alpha} \to c^{\dagger}_{n,\uparrow} c_{n,\uparrow} - c^{\dagger}_{n,\downarrow} c_{n,\downarrow} + 1 = 2S^{z}(n) + 1 \tag{6}$$

$$c_{n,\downarrow} c_{n,\uparrow} \to (-1)^{n} c^{\dagger}_{n,\downarrow} c_{n,\uparrow} = (-1)^{n} S^{+}(n). \tag{7}$$

This implies that both the spin and charge sectors of the half-filled Hubbard model are governed by the $SU(2)$ symmetry of the equivalent Heisenberg model.

On the other hand at $W < 0$, $|W| \gg t$ the PK model is equivalent to the spin-$\frac{1}{2}$ XY model [12]. The correspondence with the XY model can be seen by making the transformation

$$T^{+}_{n} = c^{\dagger}_{n,\uparrow} c^{\dagger}_{n,\downarrow} \tag{8}$$

$$T^{z}_{n} = (c^{\dagger}_{n,\uparrow} c_{n,\uparrow} + c^{\dagger}_{n,\downarrow} c_{n,\downarrow} - 1)/2. \tag{9}$$

Then the Hamiltonian becomes

$$\mathcal{H} = W \sum_{n} (T^{+}_{n} T^{-}_{n+1} + \text{h.c.}). \tag{10}$$

Electrons only appear as singlet pairs on the same site, the interaction term simply acts as a hopping term for these pairs. There is a gap in the spin excitation spectrum, the charge excitations are gapless. This picture holds true for $W \to \infty$ or $-\infty$ since the XY model is invariant with respect to a change of sign of the coupling constant. Thus, in contrast to the Hubbard model the charge sector of the PK model is governed by the $U(1)$-symmetry of the equivalent XY chain. However, it is important to note that $W \to -W$ is not a symmetry of the PK model and therefore the ground-state phase diagram is genuinely different for negative and positive W cases.

Let us now clarify peculiarities arising from the site-off-diagonal nature of the pair-hopping term. It is convenient to rewrite the corresponding interaction terms in momentum space

$$\mathcal{H}_{\text{int}} = \frac{1}{L} \sum_{k_1,k_2,k_3} V(k_1 + k_2) c^{\dagger}_{\uparrow}(k_1) c^{\dagger}_{\downarrow}(k_2) c_{\downarrow}(k_3) c_{\uparrow}(k_1 + k_2 - k_3) \tag{11}$$

where $V(k_1 + k_2) = 2W \cos(k_1 + k_2)$ in the case of PK and $V(k_1 + k_2) = U$ in the case of the Hubbard model.

In the case of weak interaction ($U, W \ll t$) only states near the two Fermi points $k_{\text{F}} = \pm\pi/2$ are relevant. Therefore, the umklapp scattering with $k_1 \sim k_2 \sim -k_3 \sim \pm\pi/2$ is the only relevant scattering process different for the Hubbard and the PK model.

In the case of attractive interaction ($U, W < 0$) the umklapp scattering is irrelevant. In this case the difference in symmetry is crucial [13]. This difference determines a very subtle (seen only in the second-order renormalization-group approximation) difference in scaling properties of the Hubbard and PK models, which, however, leads to a basic difference in the ground-state phase diagram. Due to the $U(1)$ symmetry of the charge channel the SS instability dominates in the ground state of the PK model for all $W < 0$ [13] while the $SU(2) \bigotimes SU(2)$ symmetry of the half-filled Hubbard model leads to the co-dominance of the CDW and SS correlations in the ground state at $U < 0$.

In contrast, in the case of repulsive interaction ($U, W > 0$) the umklapp scattering is relevant. Similar to the Hubbard model, in the case of the PK model it leads to the dynamical generation of a commensurability gap in the charge excitation spectrum at half-filling [13]. However this is the only similarity. As we show below, the site-off-diagonal nature of the pair-hopping term manifests itself pronouncedly in this case (via the opposite

sign of the umklapp coupling constant) and leads to a completely different symmetry of instabilities in PK and Hubbard models. This can be seen already within the first-order renormalization-group analysis. Therefore below we will restrict ourselves to this accuracy.

3. Weak-coupling renormalization-group analysis

In what follows we will study the weak-coupling ground-state phase diagram of the PKH model [16] given by the Hamiltonian

$$\mathcal{H} = -t^* \sum_{n,\alpha} (: c^\dagger_{n,\alpha} c_{n+1,\alpha} + c^\dagger_{n+1,\alpha} c_{n,\alpha} :) + U \sum_n : c^\dagger_{n,\uparrow} c_{n,\uparrow} :: c^\dagger_{n,\downarrow} c_{n,\downarrow} : + W \sum_n (: c^\dagger_{n,\uparrow} c_{n+1,\uparrow} :: c^\dagger_{n,\downarrow} c_{n+1,\downarrow} : + \text{h.c.}). \tag{12}$$

Here $t^* = t + W/\pi$ and :: denote normal ordering with respect to the ground state of noninteracting electron gas. We will restrict ourselves by considering the half-filled band case and repulsive on-site interaction ($U > 0$).

In the weak-coupling limit ($U, |W| \ll t$) the low-energy physics is controlled by states near the two Fermi points $\pm k_F$. After linearization of the spectrum around these points we obtain two species $\psi_{R,\alpha}(x)$ and $\psi_{L,\alpha}(x)$, which describe excitations with dispersion relations $E_p = \pm v_F p$, where the momentum p is measured from the corresponding Fermi point and v_F is the Fermi velocity.

The effective Hamiltonian describing the low-energy behaviour of the model (12) written in terms of continuum fields $\psi_{R,\alpha}(x)$ and $\psi_{L,\alpha}(x)$ has the form

$$\begin{aligned}\mathcal{H} = {} & -\mathrm{i} v_F \sum_\alpha \int \mathrm{d}x \, [\psi^\dagger_{R,\alpha} \partial_x \psi_{R,\alpha} - \psi^\dagger_{L,\alpha} \partial_x \psi_{L,\alpha}] \\ & + \pi v_F \int \mathrm{d}x \left\{ (-g_c \rho_R(x) \rho_L(x) - g_s \sigma_R(x) \sigma_L(x)) \right. \\ & + \sum_\alpha \tfrac{1}{2} g_\perp (\psi^\dagger_{R,\alpha}(x) \psi^\dagger_{L,-\alpha}(x) \psi_{R,-\alpha}(x) \psi_{L,\alpha}(x) + \text{h.c.}) \\ & \left. + \sum_\alpha \tfrac{1}{2} g_u (\psi^\dagger_{R,\alpha}(x) \psi^\dagger_{R,-\alpha}(x) \psi_{L,-\alpha}(x) \psi_{L,\alpha}(x) + \text{h.c.}) \right\}. \end{aligned} \tag{13}$$

Here

$$\rho_{R(L)} = \frac{1}{\sqrt{2}} \sum_\alpha \psi^\dagger_{R(L),\alpha}(x) \psi_{R(L),\alpha}(x) \tag{14}$$

$$\sigma_{R(L)} = \frac{1}{\sqrt{2}} \sum_\alpha \alpha \psi^\dagger_{R(L),\alpha}(x) \psi_{R(L),\alpha}(x) \tag{15}$$

and the small dimensionless coupling constants are given by

$$g_s = g_\perp = (U + 2W)/\pi v_F \tag{16}$$

$$g_c = -(U + 2W)/\pi v_F \qquad g_u = (U - 2W)/\pi v_F. \tag{17}$$

In obtaining (13), terms corresponding to scattering processes in the vicinity of a Fermi point which lead to a renormalization of the Fermi velocities in second order in g were omitted. Neglecting these terms results in a complete decoupling of charge and spin degrees of freedom. The most convenient way to analyse the model in this case is to use the bosonization procedure and convert the continuum Hamiltonian (13) to a quantum

theory of two independent Bose fields $\varphi_c(x)$ and $\varphi_s(x)$ corresponding to the charge and spin degrees of freedom. The corresponding maping formulae are [26]

$$\psi_{R,\alpha} \to \frac{1}{\sqrt{2\pi a_0}} \exp\left(\mathrm{i}\sqrt{\pi/2}[\varphi_c(x) + \bar{\varphi}_c(x) + \alpha(\varphi_s(x) + \bar{\varphi}_s(x))]\right) \tag{18}$$

$$\psi_{L,\alpha} \to \frac{1}{\sqrt{2\pi a_0}} \exp\left(-\mathrm{i}\sqrt{\pi/2}[\varphi_c(x) - \bar{\varphi}_c(x) + \alpha(\varphi_s(x) - \bar{\varphi}_s(x))]\right). \tag{19}$$

Here $\partial_x \bar{\varphi}_{c(s)} = -P_{c(s)}$ where $P_{c(s)}(x)$ is the momentum conjugate to $\varphi_{c(s)}(x)$ and a_0 is a cut-off parameter of the order of the lattice constant.

Using relations (18) and (19), after rescaling the fields and lengths the Hamiltonian (13) acquires the following form

$$\mathcal{H} = \mathcal{H}_c + \mathcal{H}_s \tag{20}$$

$$\mathcal{H}_c = \int \mathrm{d}x \left\{ \frac{v_c}{2}[(\partial_x \varphi_c)^2] + P_c^2(x) + \frac{m_c}{\pi \alpha_0^2} \cos(\beta_c \varphi_c(x)) \right\} \tag{21}$$

$$\mathcal{H}_s = \int \mathrm{d}x \left\{ \frac{v_s}{2}[(\partial_x \varphi_s)^2] + P_s^2(x) + \frac{m_s}{\pi \alpha_0^2} \cos(\beta_s \varphi_s(x)) \right\} \tag{22}$$

where

$$m_c = -\frac{1}{2\pi} g_u \qquad \beta_c^2 = 8\pi(1 + \tfrac{1}{2} g_c) \tag{23}$$

$$m_s = \frac{1}{2\pi} g_\perp \qquad \beta_s^2 = 8\pi(1 + \tfrac{1}{2} g_s). \tag{24}$$

The infrared behaviour of the sine-Gordon Hamiltonian $\mathcal{H}_{c,s}$ is described by the corresponding pair of renormalization-group equations for the effective coupling constants Γ_i [27]

$$\begin{aligned} \mathrm{d}\Gamma_u/\mathrm{d}L &= -\Gamma_c \Gamma_u \\ \mathrm{d}\Gamma_c/\mathrm{d}L &= -\Gamma_u^2 \end{aligned} \tag{25}$$

$$\begin{aligned} \mathrm{d}\Gamma_\perp/\mathrm{d}L &= -\Gamma_s \cdot \Gamma_\perp \\ \mathrm{d}\Gamma_s/\mathrm{d}L &= -\Gamma_\perp^2 \end{aligned} \tag{26}$$

where $L = \ln(a_0)$ and $\Gamma_i(0) = g_i$. Each pair of equations (25) and (26) describes the Kosterlitz–Thouless transition [28] in charge and spin channels. For $g_c \geqslant |g_u|$ ($g_s \geqslant |g_\perp|$) we have a weak coupling regime; the effective mass $M_{c(s)} \to 0$, indicating the gapless character of the corresponding charge (spin) excitations in this case. For $g_c < |g_u|$ ($g_s < |g_\perp|$) the system scales into a strong coupling regime; depending on the sign of the bare mass $m_{c(s)}$, the effective mass $M_{c(s)} \to \pm\infty$, which signals the crossover into a strong coupling regime and indicates the dynamical generation of a commensurability gap in the charge (spin) excitation spectrum. The fields $\varphi_c(\varphi_s)$ get ordered with the vacuum expectation values [29]

$$\langle \varphi_{c(s)} \rangle = \frac{\pi}{\beta_{c(s)}} \qquad (m_{c(s)} > 0) \tag{27}$$

$$\langle \varphi_{c(s)} \rangle = 0 \qquad (m_{c(s)} < 0). \tag{28}$$

The ordering of these fields determines the symmetry properties of the possible ordered ground states of the fermionic system.

Using equations (16), (17) and (23) one easily finds that at all $U + 2W > 0$ $M_s \to 0$. Therefore the spin excitation spectrum of the repulsive PK model ($W > 0, U = 0$) as well as of the repulsive Hubbard model ($U > 0, W = 0$) are gapless. The spin excitation

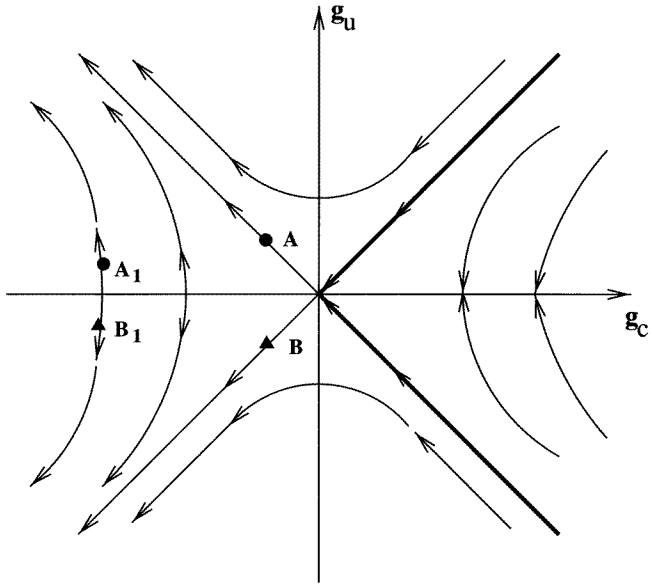

Figure 1. The renormalization-group flow diagram; the arrows denote the direction of flow with increasing length scale. The black dots correspond to the starting points for the $U > 0$ Hubbard model (A) and the PKH model at $0 < W < U/2$ (A_1). The triangles correspond to the starting points for the $W > 0$ PK model (B) and the PKH model at $W > U/2$ (B_1).

spectrum is gapped at $U + 2W < 0$. In this sector the φ_s field gets ordered with vacuum expectation value $\langle\varphi_s\rangle = 0$.

On the other hand, at all $U + 2W > 0$ $|M_c| \to \infty$ and there is a gap in the charge excitation spectrum. However, depending on the bare value of the charge mass m_c (i.e. umklapp term) the scaling trajectories stay in different sectors of the phase diagram (see figure 1). At $U > 2W$ ($m_c < 0$) $M_c \to -\infty$ and the φ_c field gets ordered with vacuum expectation value $\langle\varphi_c\rangle = 0$. Thus in the case of the repulsive Hubbard model ($W = 0, U > 0$) $\langle\varphi_c\rangle = 0$. At $2W > U > 0$ ($m_c > 0$) $M_c \to \infty$ and the φ_c field gets ordered with vacuum expectation value $\langle\varphi_c\rangle = \pi/\beta_c$. Therefore in the case of the repulsive PK model ($U = 0, W > 0$) $\langle\varphi_c\rangle = \pi/\beta_c$. As we show below this leads to essentially different symmetries of instabilities in the ground state of the Hubbard and PK models.

4. Correlation functions

To clarify the symmetry properties of the ground states of the system in different sectors we use, besides the usual order parameters describing the short wavelength fluctuations of the site-located charge- and spin-density

$$O_{\mathrm{CDW}} = (-1)^n \sum_\alpha c^\dagger_{n,\alpha} c_{n,\alpha} = \sum_\alpha (\psi^\dagger_{R,\alpha}\psi_{L,\alpha} + \mathrm{h.c.})$$
$$\sim \sin(\tfrac{1}{2}\beta_c\varphi_c)\cos(\tfrac{1}{2}\beta_s\varphi_s) \tag{29}$$
$$O^z_{\mathrm{SDW}} = (-1)^n \sum_\alpha \alpha c^\dagger_{n,\alpha} c_{n,\alpha} = \sum_\alpha \alpha(\psi^\dagger_{R,\alpha}\psi_{L,\alpha} + \mathrm{h.c.})$$
$$\sim \cos(\tfrac{1}{2}\beta_c\varphi_c)\sin(\tfrac{1}{2}\beta_s\varphi_s) \tag{30}$$

$$O^x_{\rm SDW} = (-1)^n \sum_\alpha c^\dagger_{n,\alpha} c_{n,-\alpha} = \sum_\alpha (\psi^\dagger_{R,\alpha}\psi_{L,-\alpha} + \psi^\dagger_{L,\alpha}\psi_{R,-\alpha})$$
$$\sim \cos(\tfrac{1}{2}\beta_c\varphi_c)\cos(\tfrac{1}{2}\bar\beta_s\bar\varphi_s) \tag{31}$$
$$O^y_{\rm SDW} = {\rm i}(-1)^n \sum_\alpha \alpha c^\dagger_{n,\alpha} c_{n,-\alpha} = -{\rm i}\sum_\alpha \alpha(\psi^\dagger_{R,\alpha}\psi_{L,-\alpha} + \psi^\dagger_{L,\alpha}\psi_{R,-\alpha})$$
$$\sim \cos(\tfrac{1}{2}\beta_c\varphi_c)\sin(\tfrac{1}{2}\bar\beta_s\bar\varphi_s) \tag{32}$$

an additional set of order parameters describing the short wavelength fluctuations of the bond-located charge- and spin-density [30]

$$O_{Bd\text{-CDW}} = (-1)^n \sum_\alpha (c^\dagger_{n,\alpha} c_{n+1,\alpha} + c^\dagger_{n+1,\alpha} c_{n,\alpha}) = -{\rm i}\sum_\alpha (\psi^\dagger_{R,\alpha}\psi_{L,\alpha} - {\rm h.c.})$$
$$\sim \cos(\tfrac{1}{2}\beta_c\varphi_c)\cos(\tfrac{1}{2}\beta_s\varphi_s) \tag{33}$$
$$O^z_{Bd\text{-SDW}} = (-1)^n \sum_\alpha \alpha(c^\dagger_{n,\alpha} c_{n+1,\alpha} + c^\dagger_{n+1,\alpha} c_{n,\alpha}) = -{\rm i}\sum_\alpha \alpha(\psi^\dagger_{R,\alpha}\psi_{L,\alpha} - {\rm h.c.})$$
$$\sim \sin(\tfrac{1}{2}\beta_c\varphi_c)\sin(\tfrac{1}{2}\beta_s\varphi_s) \tag{34}$$
$$O^x_{Bd\text{-SDW}} = (-1)^n \sum_\alpha (c^\dagger_{i,\alpha} c_{i+1,-\alpha} + {\rm h.c.}) = {\rm i}\sum_\alpha (\psi^\dagger_{R,\alpha}\psi_{L,-\alpha} - \psi^\dagger_{L,\alpha}\psi_{R,-\alpha})$$
$$\sim \sin(\tfrac{1}{2}\beta_c\varphi_c)\cos(\tfrac{1}{2}\bar\beta_s\bar\varphi_s) \tag{35}$$
$$O^y_{Bd\text{-SDW}} = {\rm i}(-1)^n \sum_\alpha \alpha(c^\dagger_{i,\alpha} c_{i+1,-\alpha} + {\rm h.c.}) = \sum_\alpha \alpha(\psi^\dagger_{R,\alpha}\psi_{L,-\alpha} - \psi^\dagger_{L,\alpha}\psi_{R,-\alpha})$$
$$\sim \sin(\tfrac{1}{2}\beta_c\varphi_c)\sin(\tfrac{1}{2}\bar\beta_s\bar\varphi_s) \tag{36}$$

where $\bar\beta_s = 8\pi/\beta_s$

Using equations (29)–(36) and the vacuum values of the field φ_ρ and φ_s one obtains (cf [29]) the phase diagram of the model. Let us first consider the limiting cases.

The Hubbard model ($W = 0, U > 0$). The vacuum expectation value $\langle\varphi_c\rangle = 0$. Using equations (29)–(36) one recovers the well-known phase diagram. The SDW and Bd-CDW instabilities survive. Due to the gapless character of spin excitations, the corresponding correlations show a power-law decay at large distances

$$\langle O_{Bd\text{-CDW}}(x) O_{Bd\text{-CDW}}(x')\rangle \sim |x - x'|^{-1} \tag{37}$$
$$\langle O^{(j)}_{\rm SDW}(x) O^{(j)}_{\rm SDW}(x')\rangle \sim |x - x'|^{-1} \qquad j = x, y, z \tag{38}$$

with the critical indices governed by the $SU(2)$-symmetry of the model. The Bd-CDW correlations describe the Peierls instability in the system. Coexistence of the SDW and Bd-CDW instabilities in the repulsive Hubbard model is the mechanism of the spin–Peierls transition at $U \gg t$.

In the case of the PK model ($U = 0$) the vacuum expectation value $\langle\varphi_c\rangle = \pi/\beta_c$. This implies complete suppression of the SDW and Bd-CDW instabilities. In this case the CDW and Bd-SDW correlations show an identical power-law decay at large distances

$$\langle O_{\rm CDW}(x) O_{\rm CDW}(x')\rangle \sim |x - x'|^{-1} \tag{39}$$
$$\langle O^{(j)}_{Bd\text{-SDW}}(x) O^{(j)}_{Bd\text{-SDW}}(x')\rangle \sim |x - x'|^{-1} \qquad j = x, y, z. \tag{40}$$

Once again the critical indices are determined by the $SU(2)$-spin symmetry of the PK model.

As we see the symmetry of correlations in the half-filled $W > 0$ PK model is essentially different from the half-filled repulsive Hubbard model. Besides the CDW-type instability [14], an unusual magnetic instability (Bd-SDW) corresponding to a staggered magnetization located on bonds between the sites is most divergent in the ground state of the PK model.

Possibility for Bd-SDW ordering is a direct consequence of the site-off-diagonal nature of the pair-hopping interaction.

In the weak-coupling continuum limit Hamiltonian (13) the difference between the on-site and pair-hopping interaction manifest itself only via the opposite sign of the umklapp coupling constant. The chiral transformation $\psi_{L,\alpha} \rightarrow -\mathrm{i}\psi_{L,\alpha}$ changes the sign of the umklapp term, while leaving other couplings unchanged. As it follows from equations (29)–(36) this transformation interchanges the on-site and on-bond order parameters. Therefore, although after this transformation continuum-limit versions of the Hubbard and PK model are equivalent with $U \rightarrow 2W$, the character of instabilities is completely different.

5. Phase diagram of the Penson–Kolb–Hubbard model

On the basis of the results presented in the previous sections we can now discuss the ground-state phase diagram of the half-filled PKH model. In the case of $W < 0$ the model was studied by Hui and Doniach [16] using exact diagonalization data for systems of up to 12 sites and renormalization-group analysis. Later Bhattacharyya and Roy [14] investigated the ground-state phase diagram using the real-space renormalization-group method. Recently the model was analysed within the Green function formalism by Belkasri and Buzatu [18]. In all the previous studies the possibility for the bond-located ordering was not considered. Below we will sketch out the ground-state phase diagram focusing our attention on the new ordered phases. Although our results are valid in the weak-coupling limit ($U, |W| \leqslant t$) we believe that the new states will remain at ($U, |W| \geqslant t$).

The ground-state phase diagram consists of five sectors (see figure 2). At $U > 2|W|$ (sector A) the on-site repulsion dominates: there is a gap in the charge excitation spectrum, the spin excitation spectrum is gapless and the SDW and Bd-CDW instabilities are most divergent in the ground state. At $U = 2|W|$ the transition into a regime where the on-bond correlations dominate takes place.

In the case of $W > 0$ the transition line $U = 2W$ corresponds to a metallic state. After the transition, at $U < 2W$ (sector B) the excitation spectrum is similar to the $U > 2W$ case. There is a gap in the charge excitation spectrum, the spin excitation spectrum is

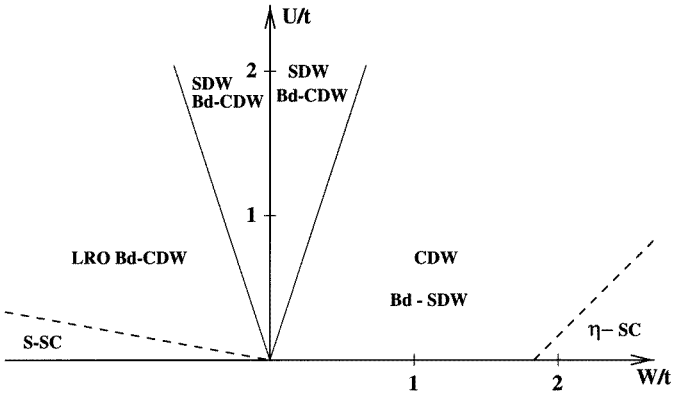

Figure 2. Phase diagram of the one-dimensional PKH model for half-filling. SDW: spin-density-wave; CDW: charge-density-wave; Bd-CDW: dimerized phase; Bd-SDW bond-located SDW phase; Bd-CDW LRO: dimerized phase with true long-range order; S-SC: singlet superconducting phase; η-SC: local pair superconducting phase with pairs of centre-off-mass momentum π.

gapless. However, in this phase the symmetry of instabilities is different. The CDW and Bd-SDW instabilities are most divergent in the ground state. This phase remains in the case of PK model ($U = 0$) at $W < W_c = 1.8t$ where at $W = W_c$ the transition into an η-superconducting phase (sector C) takes place [14, 15]. For $U \neq 0$ W_c increases linearly with U [14, 31].

At $W < 0$ the situation is different. In this case at $U < 2|W|$ (sector D) the spin gap opens, the φ_s field gets ordered with vacuum expectation value $\langle\varphi_s\rangle = 0$. The state is characterized by the gapped charge and spin excitation spectrum. The Bd-CDW correlations show a true long-range order. In this case the dimerized phase is realized. Note that this transition into the dimerized state differs from the stardard CDW–SDW transition along the $U = 2V$ line in the extended Hubbard model with nearest-neighbour V repulsion [32]. In the latter case the charge gap vanishes along the $U = 2V$ in the case of weak couplings. The Peierls phase becomes unstable with respect to transition into the singlet superconducting phase at $U = 0$. However, this is an artefact of the approximation used. Second-order renormalization-group studies show that the superconducting phase penetrates into the region with $U > 0$ [16, 14] (sector E). In contrast to previous studies [16, 14, 18] our results indicate that the dimerized state, but not the SDW or CDW phases, is unstable with respect to transition into the SS phase with increasing $|W|$.

In summary, in this paper we presented the weak-coupling phase diagram for the one-dimensional half-filled PKH model at $U > 0$ and arbitrary W. For $W > 0$ we compared the low-energy behaviours of the repulsive Hubbard model ($U > 0, W = 0$) and the repulsive PK model ($U = 0, W > 0$). We have shown that, despite the similar excitation spectra, the character of instabilities in these models is completely different. If the Hubbard model is characterized by the coexistence of SDW and Peierls instabilities, in the $W > 0$ PK model CDW and Bd-SDW instabilities are most divergent. The Bd-SDW is an unconvential insulating magnetic phase, characterized by a gapless spin excitation spectrum and a staggered magnetization located on bonds between sites. The possibility of bond-located ordering results from the site-off-diagonal nature of the pair-hopping term and is a special feature of the half-filled band case. The transition from the phase with dominating on-site repulsion (SDW, Bd-CDW) into the phase with dominating pair-hopping interaction takes place along the line $U = 2W$. At $U = 2W$ the PKH model shows metallic properties. In the case of $W < 0$, $U < 2|W|$ the dimerized phase is realized. This phase becomes unstable to transition into a singlet superconducting phase with increasing $|W|$.

Acknowledgments

GJ gratefully acknowledges Professor N Dombey for hospitality and many useful discussions during his stay in the Sussex University where part of this work was done. He also acknowledges the support of the INTAS grant N 94-3862. Research was performed within the programme of the Sonderforschungsbereich 341 supported by the Deutsche Forschungsgemeinschaft.

References

[1] See for review Micnas R, Ranninger J and Robaszkiewicz S 1990 *Rev. Mod. Phys.* **62** 113
[2] Yang C N 1989 *Phys. Rev. Lett.* **63** 2144
[3] Yang C N 1962 *Rev. Mod. Phys.* **34** 694
[4] Sewell G L 1995 *J. Stat. Phys.* **61** 415
[5] Nieh H T, Su G and Zhao B M 1995 *Phys. Rev.* B **51** 3760

[6] Singh R R P and Scalletar R T 1991 *Phys. Rev. Lett.* **66** 3203
[7] Eßler F H L, Korepin V E and Schoutens K 1992 *Phys. Rev. Lett.* **68** 2960
[8] Eßler F H L, Korepin V E and Schoutens K 1993 *Phys. Rev. Lett.* **70** 73
[9] de Boer J, Korepin V E and Schadschneider A 1995 *Phys. Rev. Lett.* **74** 789
[10] de Boer J and Schadschneider A 1995 *Phys. Rev. Lett.* **75** 4298
[11] Schadschneider A 1995 *Phys. Rev.* B **51** 10 386
[12] Penson K A and Kolb M 1986 *Phys. Rev.* B **33** 1663
Penson K A and Kolb M 1986 *J. Stat. Phys.* **44** 129
[13] Affleck I and Marston J B 1988 *J. Phys. C: Solid State Phys.* **21** 2511
[14] Bhattacharyya B and Roy G K 1995 *J. Phys.: Condens. Matter* **7** 5537
[15] Bouzerar G and Japaridze G I 1996 unpublished
[16] Hui A and Doniach S 1993 *Phys. Rev.* B **42** 2063
[17] Sikkema A E and Affleck I 1995 *Phys. Rev.* B **52** 10 207
[18] Belkasri A and Buzatu F D 1996 *Phys. Rev.* B **53** 7171
[19] van den Bossche M and Caffarel M 1996 *Phys. Rev.* B **54** 17 414
[20] Bedürftig G and Frahm H 1995 *J. Phys. A: Math. Gen.* **28** 4453
[21] Bariev R Z, Klümper A and Zittartz J 1995 *Europhys. Lett.* **32** 85
[22] Hubbard J 1963 *Proc. R. Soc.* A **276** 238
[23] Kivelson S, Su W-P, Schrieffer J R and Heeger A J 1987 *Phys. Rev. Lett.* **58** 1899
[24] Frahm H and Korepin V E 1990 *Phys. Rev.* B **52** 10 553
[25] Kawakami N and Yang S-K 1990 *Phys. Lett.* A **148** 359
[26] Schotte K D and Schotte U 1969 *Phys. Rev.* **182** 479
Luther A and Peschel I 1974 *Phys. Rev.* B **9** 2911
[27] Wiegmann P 1978 *J. Phys. C: Solid State Phys.* **11** 1583
[28] Kosterlitz J M and Thouless D 1973 *J. Phys. C: Solid State Phys.* **6** 1181
[29] Muttalib K A and Emery V J 1986 *Phys. Rev. Lett.* **57** 1370
Giamarchi T and Schulz H J 1988 *Phys. Rev.* B **33** 2066
[30] Nersesyan A A 1991 *Phys. Lett.* A **153** 49
[31] Bouzerar G 1996 unpublished
[32] Cannon J W and Fradkin E 1990 *Phys. Rev.* B **41** 9435